Available online at www.sciencedirect.com
SCIENCE DIRECT
Polymer 46 (2005) 5183–5193
polymer
www.elsevier.com/locate/polymer

Thermoplastic polyurethane nanocomposites of reactive silicate clays: effects of soft segments on properties

Asim Pattanayak[1], Sadhan C. Jana*

Department of Polymer Engineering, College of Polymer Science and Engineering, University of Akron, Akron, OH 44325-0301, USA

Received 15 December 2004; received in revised form 31 March 2005; accepted 11 April 2005

Abstract

This paper addresses the effects of soft-segment on clay particle exfoliation and resultant mechanical and thermal properties of nanocomposites of reactive layered silicate clay and thermoplastic polyurethanes (TPU). The composites were synthesized via a two-step bulk polymerization scheme from polyether- and polyesterpolyols of molecular weight 2000, diphenylmethanediisocyanate, butanediol, and up to 5 wt% reactive layered silicate clay. It was found that the extent of tethering reactions between polymer chains carrying residual –NCO groups and reactive clay particles was significant, although did not depend on the nature of polyol used. Nanocomposites were obtained only in the case of polyesterpolyol, which can be attributed to both clay–polymer reactions and higher viscosity in the clay–polymer mixing step. These nanocomposites showed 125% increase in tensile stress, 100% increase in elongation, and 78% increase in tensile modulus along with 130% increase in tear strength and a 60% reduction in volume loss in abrasion test. It was observed that hydrogen bonding did not influence the properties and the extent of hydrogen bonding was not affected by the clay particles.

Keywords: Reactive clays; Nanocomposites; Exfoliation

1. Introduction

Wang and Pinnavaia [1] reported the first work on composites of polyurethanes and organically treated layered silicate clays and showed that large enhancement in tensile strength and tensile modulus are possible even with intercalated clay particles. This was followed by a spate of research activities on the synthesis of clay composites of thermoplastic polyurethanes (TPU) via solution and bulk polymerization methods [2–19]. In a majority of these studies, clay particles were intercalated by soft segment polyols prior to reaction with isocyanates, drawing a parallel to the successful in situ polymerization scheme for polyamide–clay nanocomposites [20,21]. Tien and Wei [7,11] synthesized clay–tethered polyurethane nanocomposites in solutions in *N*,*N*′-dimethylformamide (DMF) by allowing prepolymers with –NCO end groups to react with organic ammonium ions carrying between one and three $–CH_2OH$ groups. Osman et al. [19] prepared polyurethane adhesive nanocomposites in solution and found substantial reduction in permeability of oxygen and water vapor due to partially exfoliated clay particles. Recently, Cao and Lee [22] prepared TPU nanocomposites of reactive clay by planting tin catalyst molecules in the clay galleries and exploiting intra-gallery polymerization, similar to what was done in the development of polyamide–clay nanocomposites [20,21].

Recently, [23] we reported two bulk polymerization methods for the synthesis of clay–tethered TPU nanocomposites of polyetherpolyol of molecular weight ~1000. In both methods, polymer chains carrying –NCO end groups were allowed to react with $–CH_2CH_2OH$ groups of quaternary ammonium ions in clay. Both high viscosity and clay–polymer reactions were found necessary for exfoliation of clay particles. Evidences of clay–polymer reactions and the extent of clay–polymer tethering were also reported. It was also reported [24] that mechanical properties of these composites were largely dictated by the clay–tethered polymer chains—an increase of 110% in tensile modulus and 160% in tensile strength over pristine polyurethane were observed. It was seen that hydrogen

* Corresponding author. Tel.: +1 330 972 8293; fax: +1 330 258 2339.
E-mail address: janas@uakron.edu (S.C. Jana).
[1] Presently at GE Global Research, Bangalore, India.

0032-3861/$ - see front matter © 2005 Elsevier Ltd. All rights reserved.
doi:10.1016/j.polymer.2005.04.035

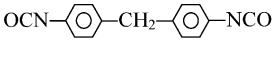

Diphenylmethane diisocyanate (MDI)

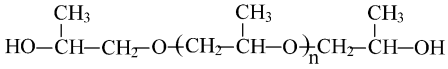

Polyether polyol

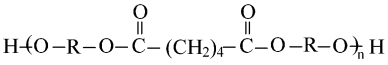

Polyester polyol with R≡CH_2CH_2-O-CH_2CH_2-

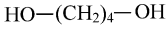

1,4 Butanediol

Fig. 1. Chemical structures of ingredients used in synthesis of polyurethane chains.

bonding between polymer chains and between polymer chains and –CH_2CH_2OH groups on clay particles had insignificant influence on mechanical properties. The extent of reaction between reactive clay and prepolymer chains and the molar ratio of –NCO and –OH have been utilized to design polyurethane nanocomposite products offering significant increases in tensile strength, but with almost no changes in tensile modulus [25].

In the present study, we investigated the effects of polyether and polyester soft segments on clay exfoliation and on resultant mechanical and thermal properties of the composite materials. We also analyzed the influence of clay particles on hydrogen bonding and thermal stability of polymer. In typical polyurethanes, hydrogen bonds are formed between hard segments via –NH groups in urethane linkages and between hard and soft segments via –NH and soft segment ether or carbonyl groups [26–35]. The interchain hydrogen bonding exerts strong influence on the rheological behavior of polyurethanes [35–37]. Yoon and Han [35] observed profound influence of isothermal annealing on dynamic storage (G') and loss modulus (G'') values. Several studies reported thermal degradation of ester- and ether-based polyurethanes [32,33,37]. Better thermal and oxidative stabilities were found in dry ester-based TPUs than ether-based TPUs. The polyester based polyurethanes exhibit equally rapid degradation in air and nitrogen, indicating that a nonoxidative mechanism was involved [38]. In contrast, the improved thermal stability of ether-based TPUs under vacuum and in nitrogen indicates that oxidative process plays a major role in the decomposition.

Table 1
Mole ratio of various components

Material	Clay content (wt%)	MDI/polyol/BD/OH from clay
Pristine polyurethane	0	2/1/1/0
With Cloisite 30B	1	2/1/0.98/0.02
	3	2/1/0.96/0.04
	5	2/1/0.93/0.07

2. Experimental

2.1. Materials and preparation method

The soft segments of thermoplastic polyurethane (TPU) was synthesized from two types of polyol—polyether type, ARCOL (PPG2000, mol. wt. 2000, Bayer Polymers, USA) and polyester type, Lexorez®1100-55 (mol. wt. 2000, Inolex Chemical Company, USA), the chemical structure of which are shown in Fig. 1. The hard segments were synthesized from diphenylmethane diisocyanate (MDI, Bayer Mondur M, mol. wt. 250, T_m = 39 °C) and 1,4-butanediol (BD, Fisher Scientific). A catalyst, dibutyltin-laureate (DABCO 120, Aldrich) was used to expedite chain extension reactions between the prepolymer and BD.

The reactive clay, Cloisite®30B containing 90 mequiv./100 g clay of quaternary ammonium ions, was kindly donated by Southern Clay Products (Gonzales, TX, USA). The quaternary ammonium ion has a structure, $N^+(CH_2CH_2OH)_2(CH_3)T$, with T representing an alkyl group of approximately 65% $C_{18}H_{37}$, 30% $C_{16}H_{33}$, and 5% $C_{14}H_{29}$ [39]. Note that –CH_2CH_2OH groups of Cloisite®30B were reactive to the isocyante end groups [7,23]. The clay particles inherently contained approximately 2 wt% moisture, which was removed by drying in vacuum oven at 80 °C for 24 h. Dried clay particles were stored in a desiccator. However, during experiments, approximately 5 min were elapsed in weighing of clay particles. The clay particles reabsorbed approximately 0.29 wt% moisture at room temperature in a room with 50% relative humidity during this period.

The base TPU was synthesized with a 2:1:1 mole ratio of MDI, polyol, and BD and contained 22 wt% hard segments. The amounts of –CH_2CH_2OH groups present in Cloisite®30B clay were taken into consideration while balancing the molar ratio of –NCO and –OH groups to 1:1 (Table 1) in clay composites. The clay contents in composites were 1, 3, and 5 wt%, which translated respectively to 0.76, 2.3, and 3.8 wt% organic-free clay.

The TPU-clay composites were synthesized as follows. The prepolymer was prepared in nitrogen atmosphere by reacting 2 mol of MDI with 1 mol of polyol at 80 °C in a round bottom flask with continuous stirring. The isocyanate concentration reached a constant value in approximately 2 h for polyesterpolyol and in 6 h for polyether polyol due to

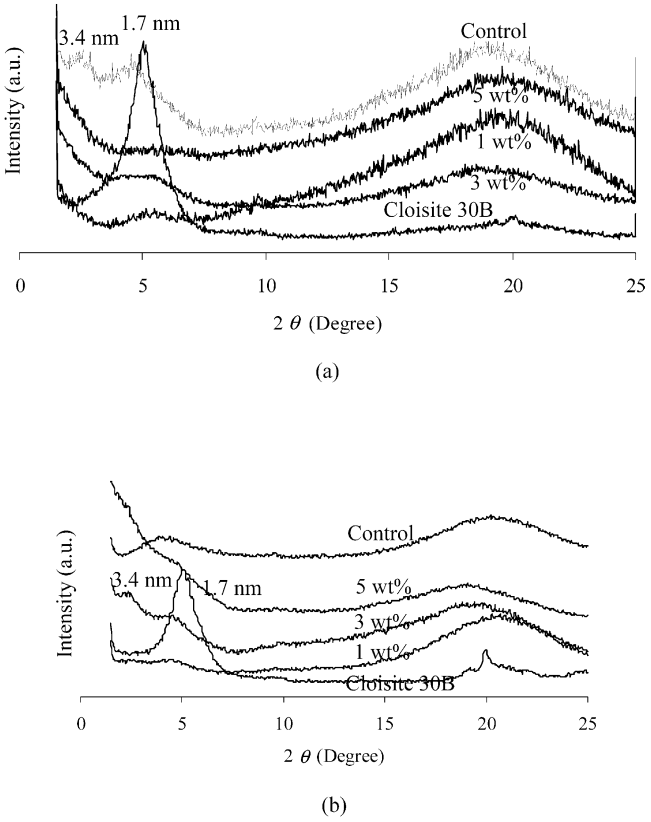

Fig. 2. WAXD patterns of nanocomposites of (a) polyether polyol and (b) polyester polyol.

slower reaction rate in the latter case. The base TPU was synthesized in Brabender Plasticoder (Model EPL 7752) batch mixer from chain extension of 1 mol prepolymer with 1 mol BD at 80 °C for 15 min in the presence of 2.3×10^{-7} mol/cm^3 dibutyltinlaureate catalyst. The polymer temperature rose to 130 °C in a few minutes and remained stable afterwards. Clay–polymer composites were prepared by adding clay particles after 6 min of chain extension reactions and further mixing of clay for approximately 9 min. Consequently, the molar ratio of –NCO and –OH groups during the chain extension step before clay addition were 1.0, 1.01, 1.02, and 1.036, respectively for TPU, and composites of 1, 3, and 5 wt% clay particles. As will be seen later, these have implications on molecular weight of polymer chains produced in each case.

'Control' materials were prepared by mixing pristine thermoplastic polyurethane synthesized with molar ratio 2:1:1 of MDI, polyol, and BD, with 5 wt% Cloisite®30B in Brabender Plastocoder at 80 °C for 9 min. The temperature also rose quickly to 130 °C in a few minutes and remained stable afterwards. The sample specimens used in mechanical testing and in X-ray characterization were prepared by compression molding at 130 °C for 5 min.

2.2. Characterization

Wide-angle X-ray diffraction (WAXD, Rigaku X-Ray, $\lambda=1.54$ Å) and transmission electron microscopy (TEM, TACNAI-12) were used to determine the state of dispersion of nanoclay structures in polymer composites. The molecular weights of clay-free polymer chains were determined by Waters 510 gel permeation chromatography (GPC) system with triple detection scheme and a polystyrene standard. A Perkin–Elmer FTIR (Model 16PC) with a resolution of 4 cm^{-1} was used to study clay–prepolymer reactions and to characterize hydrogen bonding. A Dupont DSC (Model DSC-2910) was used to study thermal transitions of polyurethane chains under nitrogen atmosphere, with a scanning rate of 20 °C/min and a temperature range of −50–250 °C. Thermo-gravimetric analysis was carried out in Dupont TGA 2950 at a scanning rate of 20 °C/min from room temperature to 800 °C. Tensile tests were performed following ASTM D 638 type V method using Instron 5567 machine with a crosshead speed of 50 mm/min. Tear properties were evaluated at room temperature with a crosshead speed of 50 mm/min using Instron device (model 5567). For this purpose, sample specimens of dimension $120\times15\times2$ mm^3 with a 4 mm deep cut were used. The abrasion resistance was determined by Zwick Abrasion Tester 6102, which is similar to DIN 53516, according to ASTM D5963. The values of various mechanical properties reported in this study represent averages of at least five samples. Dynamic mechanical thermal analysis (DMTA) was carried out by Rheometric Scientific DMTA V device with single point bending of 2 mm thick strip at a frequency of 1 Hz and heating rate of 4 °C/min from −50 to 150 °C.

3. Results and discussion

3.1. State of clay particle dispersion

The state of dispersion of clay particles can be inferred from Figs. 2 and 3. Broad diffraction peaks in Fig. 2(a) at $2\theta=5°$ (d-spacing ~1.7 nm) for each clay loading indicate the presence of Cloisite®30B particles in intercalated state in composites of polyetherpolyol. This is also evident from the existence of tactoids in TEM image in Fig. 3(a). However, no distinguishable peaks can be found between $2\theta=1.5$ and 5° in Fig. 2(b) for 5 wt% clay composites of polyesterpolyol. For other clay content, broad clay peaks ($2\theta=5°$) in the case of 1 wt% clay and a shoulder in the case of 3 wt% clay are seen in Fig. 2(b). In the case of 3 wt% clay, a peak is observed with a d-spacing of 3.4 nm, indicating that polymer chains were intercalated into clay particles. The companion TEM image in Fig. 3(b) shows exfoliated (see inset) and well-dispersed clay particles. In view of this, a true nanocomposite was produced only in the case of polyesterpolyol and 5 wt% clay. As will be discussed later, exfoliation occurred in this case due to combined effects of high shear viscosity during clay–polymer mixing and significant clay–polymer reactions as originally reported in an earlier study [23].

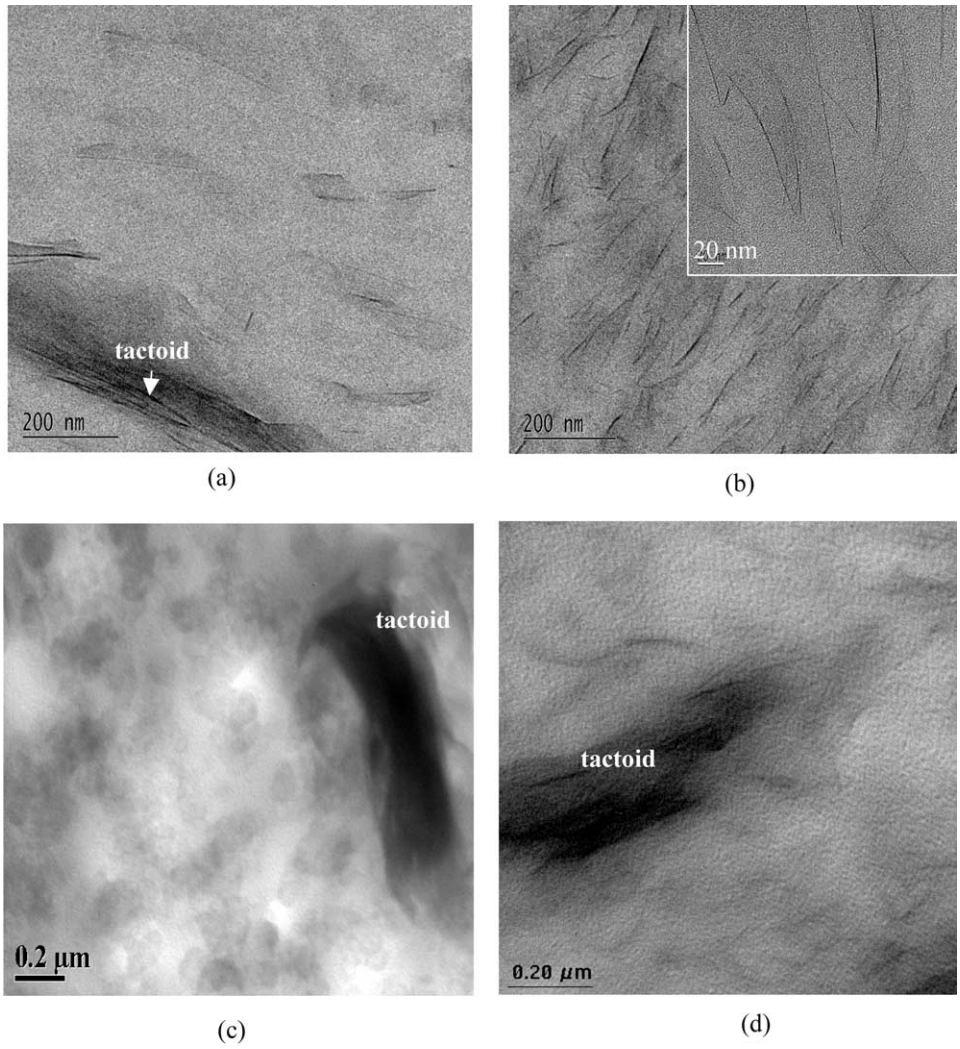

Fig. 3. TEM images of nanocomposites with (a) polyether polyol, (b) polyester polyol, (c) control composites with polyether polyol and (d) control composites with polyester polyol. In each case Cloisite®30B was 5 wt%.

The control materials obtained by mixing premade TPU with 5 wt% clay particles yielded micro-composites as revealed from WAXD patterns in Fig. 2 and TEM images in Fig. 3. The WAXD patterns in Fig. 2 show peaks corresponding to Cloisite®30B clay ($2\theta = 5.2°$) and polymer–intercalated clay (d-spacing ~ 3.4 nm). The TEM images in Fig. 3(c) and (d) show that clay particles were present as tactoids. This indicated that higher viscosity alone was not responsible for fine state of clay particle dispersion observed in Fig. 3(b). Note that chain extended TPU considered in Figs. 3(b) and 3(d) had similar viscosity, but the former contained residual –NCO groups in chain ends and the latter did not. In the rest of the paper, only the composite of polyesterpolyol and 5 wt% clay will be referred to as 'nanocomposite' and the rest will be termed 'composites'. We now analyze the reactivity between clay and polymer chains and hydrogen bonding between various segments to interpret the differences in the state of clay dispersion seen in Figs. 2 and 3.

3.2. Clay–prepolymer reaction

Our earlier study [23] established that Cloisite®30B particles participated in clay–polymer reactions via –NCO groups on chain ends and $-CH_2CH_2OH$ groups in clay. We evaluated if such reactivity was dependent on the nature of soft segments. For this purpose, Cloisite®30B particles with $-CH_2CH_2OH$ functional groups and prepolymer chains with –NCO end groups were allowed to react at 80 °C for a period of 60 min between two KBr discs. The time traces of FT-IR spectra were taken at regular intervals to monitor the absorbance due to stretching of –NCO groups at 2270 cm^{-1} and the absorbance due to carbonyl groups at 1733 cm^{-1}. The reaction mixture was prepared at room temperature by mixing prepolymer and clay particles in a ratio similar to that of a composite with 5 wt% clay.

Fig. 4(a) shows conversion (α) of the –NCO group, defined as $\alpha \equiv (A_{NCO,0} - A_{NCO})/(A_{NCO,0})$, with time. Here, A_{NCO} is the area under the peak at 2270 cm^{-1} due to –NCO

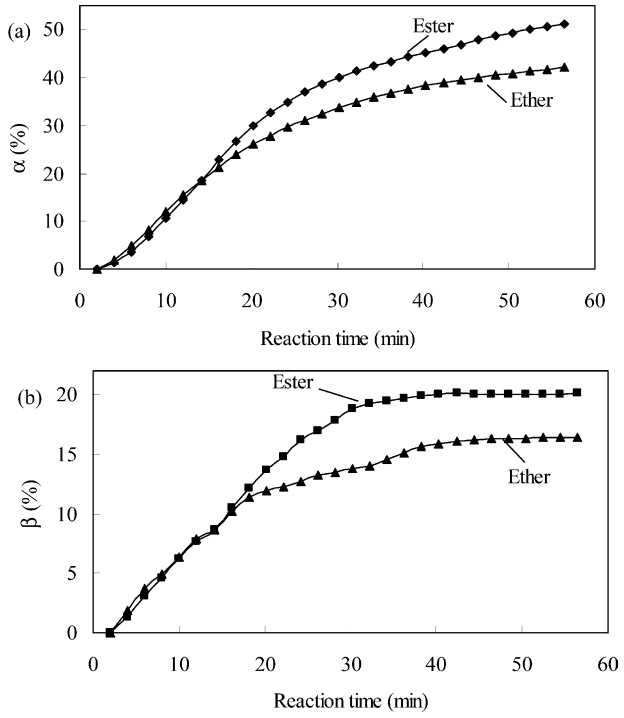

Fig. 4. Clay–prepolymer reactions at 80 °C: (a) α and (b) β vs. time.

stretching at any time t and $A_{NCO,0}$ is the initial area under the –NCO peak. The increase of carbonyl area (A_{CO}) at 1733 cm^{-1} in the form of β vs. time curves, where $\beta \equiv (A_{CO} - A_{CO,0})/(A_{CO,0})$ and $A_{CO,0}$ is the initial area under the CO peak, is shown in Fig. 4(b). Two observations can be made from Fig. 4. (1) No differences in prepolymer reactivity can be perceived up to approximately 15 min. (2) After 15 min, polyesterpolyol based prepolymer showed higher reactivity to clay. Note that the prepolymer is capable of undergoing chemical changes at the same condition giving non-zero values of α and β. However, these values were found to be much smaller than those obtained with clay [23].

In view of Fig. 4, we infer that the two types of prepolymer offered negligible differences in reactivity to clay during nanocomposite preparation. The rationale is derived from the fact that only 9 min were allowed for clay–polymer mixing, and that the data of first 15 min of clay–polymer reactions in Fig. 4 did not show any effect of the type of polyol on the values of α and β. Therefore, the same degree of clay-tethering was to be expected in both cases and the differences in clay particle dispersion seen in Figs. 2 and 3 for two type of polyol must be attributed to some other factors, for example, differences in viscosity or the extent of hydrogen bonding. It was established in our earlier study [23] in conjunction with nanocomposites of low molecular weight polyetherpolyol ($M_w \sim 1000$) that hydrogen bonding had negligible effect on clay particle exfoliation. Nevertheless, we thought that a reduced hard segment in the present study would have some effect on hydrogen bonding.

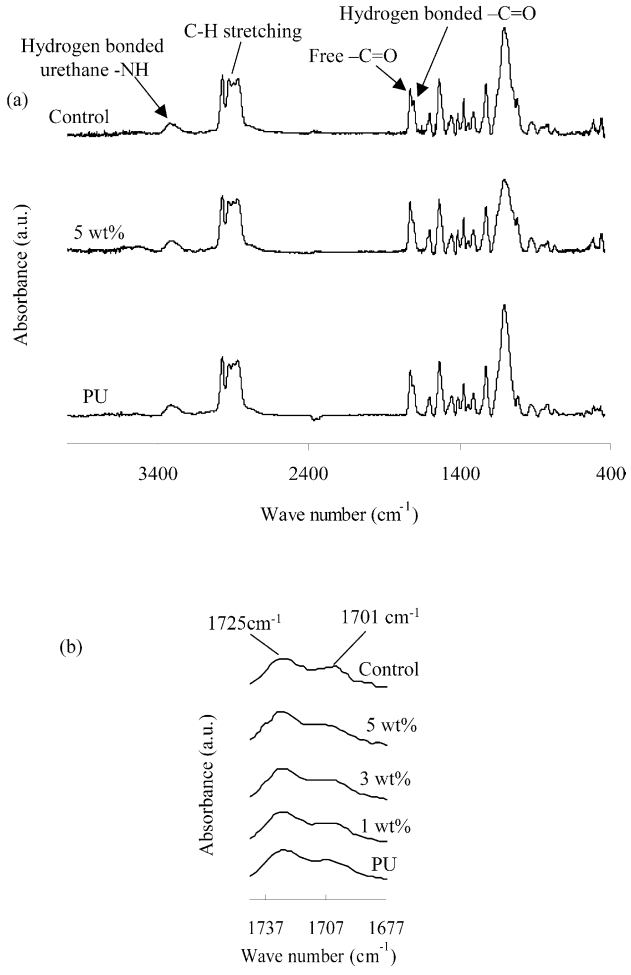

Fig. 5. (a) FT-IR spectra of composites of polyetherpolyol. (b) FT-IR spectra of carbonyl stretching.

3.3. Hydrogen bonding

FT-IR spectra of polyurethanes and their clay-composites are shown in Figs. 5 and 6. Two main regions are of interest in this study, –NH absorption and –C=O stretching. It is seen in Fig. 5(a) that the –NH absorption peak at 3320 cm^{-1} was due to hydrogen-bonded –NH groups of urethane linkages. In this case, such hydrogen bonding can be formed with hard segment carbonyl and with soft segment ether linkages. A small shoulder, seen at ~3420 cm^{-1} is characteristic of stretching of free –NH groups. The peak at 1731–1734 cm^{-1} is assigned to free urethane carbonyl, while the peak at 1715–1725 cm^{-1} is due to hydrogen bonded carbonyl. Similar assignments can be made in Fig. 6(a) for materials prepared from polyesterpolyol. The carbonyl region of polyether based TPU and its clay composites showed distinct carbonyl peaks due to free and hydrogen-bonded carbonyls, respectively at 1733 and 1703 cm^{-1}, in Fig. 5(b). This implies appreciable phase separation in the case of polyetherpolyol based TPU and its nanocomposites. However, in the case of polyester polyurethanes no distinct peaks are seen in Fig. 6(b), as the

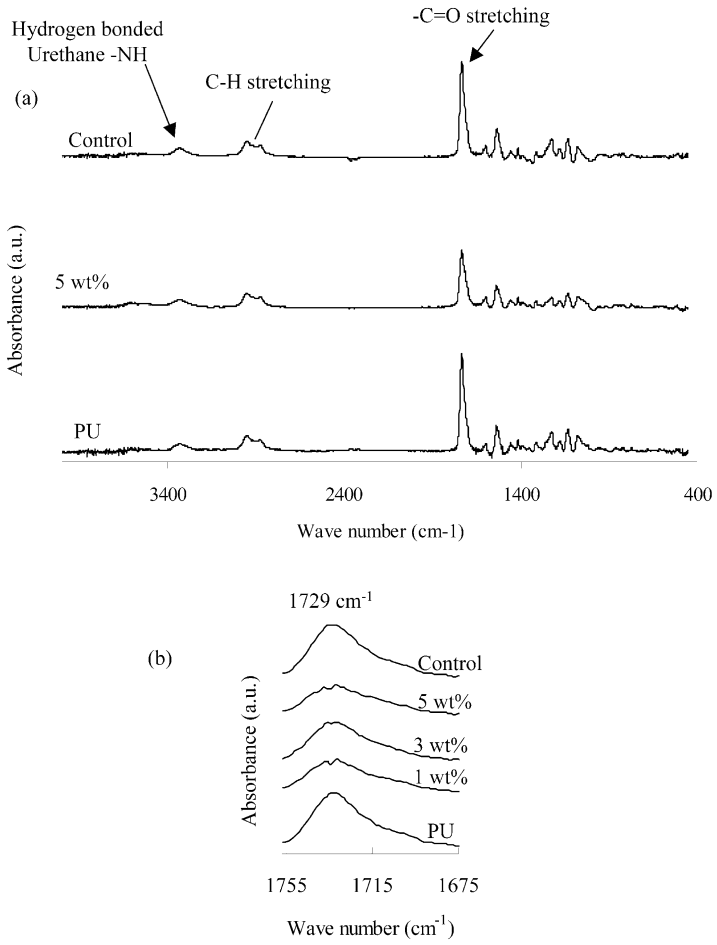

Fig. 6. (a) FTIR spectra of composites of polyester polyol and (b) FTIR spectra of carbonyl stretching.

absorptions of carbonyl groups from the ester and urethane linkages overlapped. In this case, phase mixing between hard and soft segments occurred due to increased cohesion between the hard and soft segments [32], which resulted in single prominent peak in Fig. 6(b).

The areas under hydrogen-bonded (A_{HCO}) and free carbonyl peaks (A_{CO}) were computed by curve fitting and presented in Table 2. In addition, the area under –CH stretching (2860–2940 cm^{-1}) (A_{CH}) was also computed and used as internal standard. It is seen that the values of A_{NH}/A_{CH} ratio remained almost unchanged in the presence of clay particles, indicating that clay particles did not interfere with hydrogen bond formation by urethane –NH groups. In addition, the ratio A_{HCO}/A_{CO} was insensitive to clay content for polyetherpolyol based TPU and its composites. This is contrary to what was found in our earlier study [23] – clay particles interfered with hydrogen bond formation by both –NH and –CO groups in composites of TPU based on polyetherpolyol of molecular weight ~1000. However, in that case, the hard segment content was much higher, ~36 wt%, compared to 22 wt% in the present study. The values of A_{HCO}/A_{CO} ratio for TPU of polyesterpolyol were not computed due to overlap of several peaks in carbonyl region (Fig. 6(b)).

Table 2
Ratio of the area under the peak of hydrogen-bonded –NH (A_{NH}), total C=O (A_{CO}), and –CH stretching (A_{CH}) of FTIR spectra and the ratio of area under the peak of hydrogen bonded C=O (A_{HCO}) and free C=O (A_{FCO}) groups

Material		A_{HCO}/A_{FCO}	A_{NH}/A_{CH}
With polyether polyol	PU	0.664	0.12
	1 wt%	0.604	0.15
	3 wt%	0.621	0.14
	5 wt%	0.634	0.13
	Control	0.613	0.13
With polyester polyol	PU	–	0.42
	1 wt%	–	0.47
	3 wt%	–	0.47
	5 wt%	–	0.48
	Control	–	0.43

We now turn our attention to thermal stability of TPU and it clay composites via FT-IR analysis. Specifically, we monitored the changes in area under the peaks of –NH absorption and carbonyl stretching upon increase of temperature. The composite materials, kept between two KBr discs in FT-IR set up, were allowed to equilibrate at each temperature for 5 min before FT-IR spectra was taken. In the following discussion, we include only TPU and its

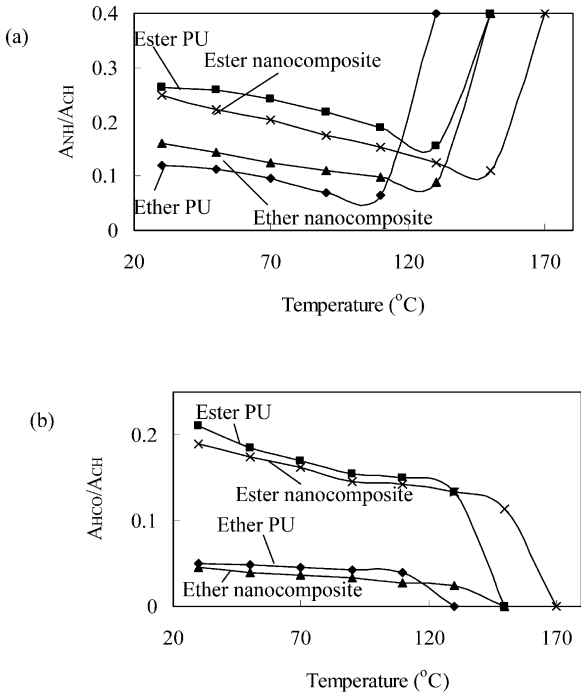

Fig. 7. Effect of temperature on stability of (a) hydrogen-bonded –NH stretching and (b) –C=O stretching.

5 wt% clay composites to establish if clay particles had any influence on the stability of TPU chains. At lower temperatures, A_{NH}/A_{CH} and A_{CO}/A_{CH} ratios show linear decrease with temperature (Fig. 7). At temperatures above 110 °C in case of polyetherpolyol and at above 150 °C in case of polyesterpolyol, the A_{NH}/A_{CH} ratio shows a sudden increase and the A_{CO}/A_{CH} ratio shows sudden a decrease. This was probably due to thermal degradation of the polymer, corroborated by a change in color from light yellow to yellowish-brown. An accepted pathway for such degradation, e.g. auto-oxidation of the diurethane bridge in the MDI structure into the quinone-imide structure, has already been reported [32]. It is evident that clay particles delayed the onset of degradation process to approximately 20 °C higher temperature.

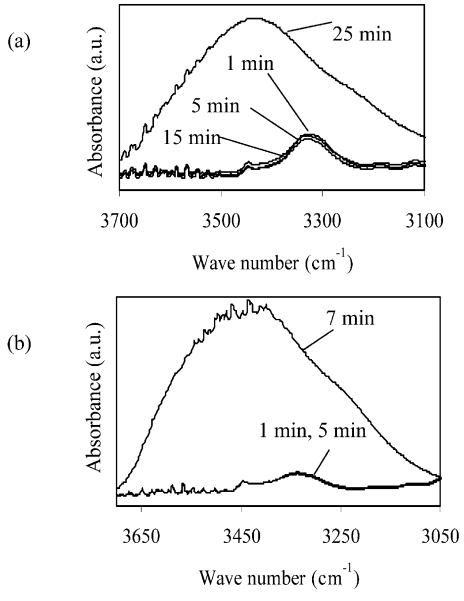

Fig. 8. Effect of temperature on area under peak due to –NH stretching.(a) 130 °C and (b) 150 °C.

This brings up an important issue related to how the composite materials were prepared. Recall that the temperature rose to 130 °C during composite preparation, which is over the stability limit for both TPU chains as revealed from the data in Fig. 7. If the results in Fig. 7 are accepted, then the materials underwent degradation at the time of preparation. To examine if such was the case, we kept a specimen of TPU of polyetherpolyol ($M_w = 2000$) between two KBr disks and subjected it to heating at 130 °C and at 150 °C. The FTIR spectra were taken in 5 min interval as seen in Fig. 8.

Fig. 8 plots only the part of spectra due to –NH absorption. It is seen that the spectra experienced a jump in absorbance after 25 min at 130 °C (Fig. 8(a)) and after 7 min at 150 °C (Fig. 8(b)). The initial –NH absorption spectra and short time spectra were, however, normal. These indicate that the materials underwent degradation only after being kept for a while between KBr discs. This also showed that the nanocomposite materials obtained in the mixing step were perfectly normal, i.e. did not have any indication of degradation. Srichatrapimuk and Cooper [32] attributed such degradation to long time exposure to infra-red radiation and possibly to catalytic effects of KBr on degradation. The FTIR data included in Fig. 7 were taken for materials kept in the FT-IR set up for at least 30 min at 130 °C. In view of this, we conclude that the material preparation method followed in this study did not cause any degradation of the materials. In stead, materials degraded after long exposure to infra-red radiation in the presence of KBr.

3.4. Fraction of clay–tethered polymer chains

Although Fig. 4 presented evidences of clay–polymer reactions, the conditions during nanocomposite preparation were different from the ones used in Fig. 4. First, the temperature of the reaction mixture was approximately 130 °C. Second, NCO group concentration was much lower. Third, catalyst was used in nanocomposite preparation while the reaction described in Fig. 4 was uncatalyzed. In view of this, we subjected the composite materials to Soxhlet extraction by tetrahydrofuran as the solvent. The objective was to recover the insoluble residue, in this case, clay–tethered polymer chains, retained by ceramic thimble of less than 0.2 μm nominal diameter. The residue was analyzed by FT-IR and DSC. In addition, the soluble polymer chain collected as extract was analyzed for molecular weight. It is readily apparent from Table 3 that the amount of residue, although increased with the amount of clay, did not depend on the type of polyol used, in line

Table 3
Soxhlet residue and weight (M_w) and number average (M_n) molecular weight of soluble polymer chains

Material		M_w	M_w/M_n	Residue; wt%
With polyether polyol	Prepolymer	6700	1.40	0
	PU	56,000	2.56	0
	1 wt%	63,000	1.70	3
	3 wt%	71,000	2.03	7
	5 wt%	80,000	1.83	10
With polyester polyol	Prepolymer	8000	1.99	0
	PU	55,000	1.91	0
	1 wt%	55,000	1.64	2
	3 wt%	79,000	1.62	6
	5 wt%	84,000	1.32	10

with equal reactivity observed in Fig. 4 for reactions between prepolymer and clay particles. Approximately 10 wt% residue obtained from the composites of 5 wt% clay particles (Table 3) reflects substantial amounts of clay–tethered polymer chains in both cases.

The FT-IR spectra of the residues in Fig. 9(a) show the characteristic peaks of –C=O group at 1725 cm^{-1}, hydrogen bonded –NH at 3307 cm^{-1}, and Si–O stretching at 1038 cm^{-1}, endorsing that polyurethane chains and clay particles were present in the residues. The DSC traces in Fig. 9(b) show sharp transitions, characteristic of soft segments of polyetherpolyol ($T_g = -34$ °C) and polyesterpolyol ($T_g = -21$ °C).

The soluble fractions of the polymer were analyzed for molecular weight as presented in Table 3. In each case, molecular weight increased with clay wt%, which can be explained on the basis of a small excess of isocyanates during chain extension reactions, e.g. –NCO to –OH molar ratio was 1.036 before addition of 5 wt% clay. Note that some of the excess –NCO groups may have formed urea linkages with –NH groups of hard segments, thus effectively producing extended chains. However, narrower molecular weight distributions seen in Table 3 in the presence of clay particles were surprising and needs thorough investigation. Such narrowing of molecular weight distribution in the presence of clay was also observed by Tien and Wei [7].

Let us revisit the issue of better clay exfoliation observed in the case of polyesterpolyol in Fig. 3(b). Note that chain extended polymers, before clay addition, had similar molecular weights, e.g. $M_w \sim 80{,}000$ for polyetherpolyol and ~84,000 for polyesterpolyol (Table 3). Also recall from the residue data in Table 3 that in each case the extent of clay–polymer tethering, measured by the amount of residue, was almost the same. However, the value of zero-shear viscosity, η measured in ARES Rheometrics rotational rheometer in parallel plate set up at 130 °C for polyesterpolyol based TPU was 3833 Pa s compared to 2467 Pa s for polyetherpolyol based TPU. Such differences in viscosity caused an appreciable differences in shear stress generated during mixing and quite possibly accounted for the differences seen in clay exfoliation between the two cases. Of course, this was aided by substantial clay–polymer reactions. Nevertheless, poor dispersion of clay in both

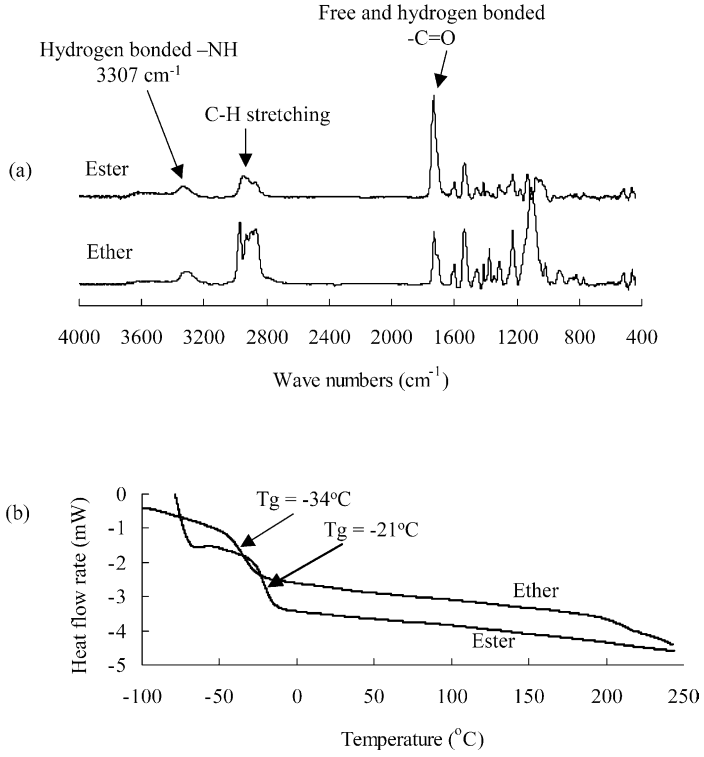

Fig. 9. (a) FT-IR spectra and (b) DSC traces of Soxhlet extracted residues of composites of 5 wt% Cloisite®30B. Ether and ester indicate respectively TPU of polyether and polyester polyol.

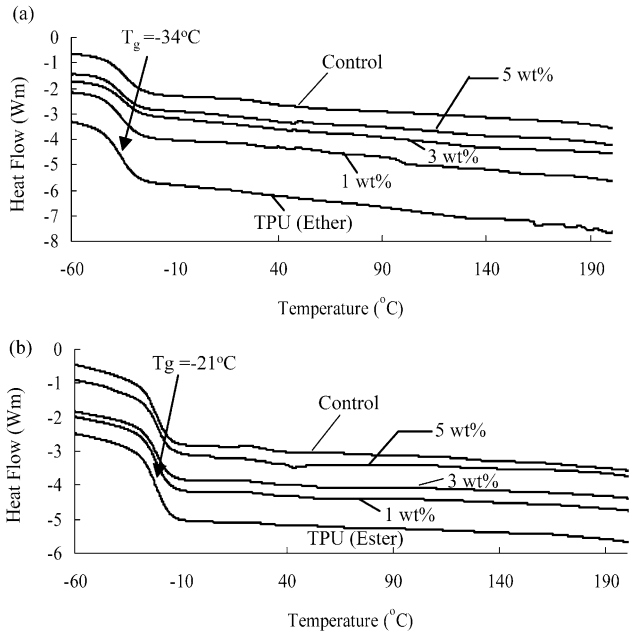

Fig. 10. DSC traces of composites of 5 wt% clay. (a) Polyether polyol and (b) polyester polyol.

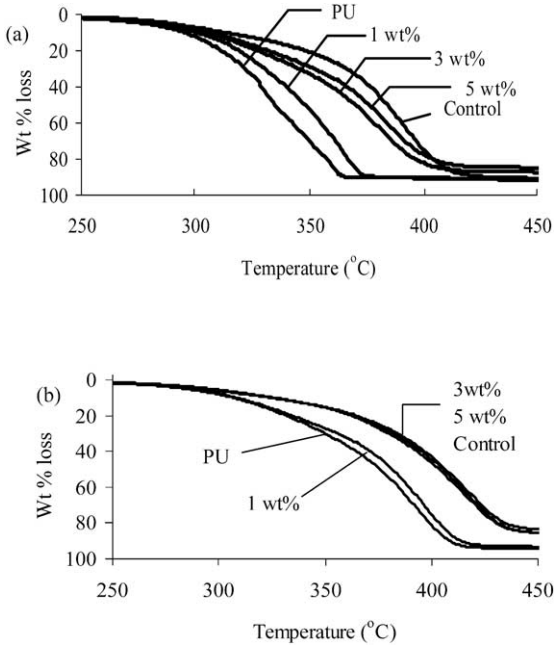

Fig. 11. Weight loss from thermo-gravimetric analysis of composites with 5 wt% clay. (a) polyether and (b) polyester polyol.

control materials (Fig. 3(c) and (d)) indicates that higher viscosity alone was not responsible for clay exfoliation in polyesterpolyol based TPU; tethering reactions between polymer chains and clay particles were also needed.

3.5. Thermal properties

The DSC traces of TPU and its composites are shown in Fig. 10 and the values of soft segment glass transition temperature (T_g) are presented in Table 4. The TPU based on polyetherpolyol had lower T_g (−35 °C) than polyester-based materials, $T_g = -21$ °C due to more flexible backbone structure of ether linkages in polyetherpolyol compared to ester type linkages. In view of Fig. 10 and Table 4, it is also evident that clay particles did not have any influence on soft segment glass transition temperature. The melting transition of the crystalline hard segments was not observed as the hard segment content was relatively low, ~22 wt%. Although clay particles did not have much influence on thermal transitions, they exerted influence on thermal stability as discussed below.

Thermogravimetric analysis in nitrogen atmosphere showed that substantial weight loss did not occur until the temperature reached approximately 280 °C for TPU as seen in Fig. 11 and Table 4. The temperature at which at least 5% weight was lost was found to be 279 and 285 °C, respectively for polyether and polyesterpolyol-based polyurethanes. The presence of 5 wt% clay increased these temperatures to respectively 289 and 296 °C, although it did not matter whether clay particles were tethered, as the control materials also exhibited the same thermal stability.

Table 4
Thermal properties

Material		T_g (°C)	T_1 (°C)[a]	T_2 (°C)[b]	Residue (%)[c]
With polyether polyol	PU	−35	279	359	0.19
	1 wt%	−35	281	364	0.79
	3 wt%	−35	285	382	2.16
	5 wt%	−33	289	382	3.47
	Control	−34	289	382	6.62
With polyester polyol	PU	−21	285	392	3.45
	1 wt%	−21	288	395	4.85
	3 wt%	−21	293	416	9.01
	5 wt%	−21	296	417	10.51
	Control	−20	296	417	10.48

[a] Temperature at 5% weight loss obtained from TGA curve.
[b] Peak temperature obtained from DTGA curve.
[c] Residue at 800 °C obtained from TGA curve.

Table 5
Storage modulus (G') at −60 °C and soft segment T_g from DMTA

Material		T_g (°C)	G'x10^9 (Pa)
With polyether polyol	PU	−23	1.81
	1 wt%	−22	1.98
	3 wt%	−21	2.29
	5 wt%	−20	2.49
	Control	−25	2.21
With polyester polyol	PU	−39	1.82
	1 wt%	−36	1.93
	3 wt%	−34	2.23
	5 wt%	−32	2.50
	Control	−37	1.93

The temperature (T_2) at which most rapid material loss occurred increased by greater than 20 °C for composites of 5 wt% clay over pristine polymer (Table 4). In addition, it can be concluded that TPU of polyesterpolyol are more stable than TPU of polyetherpolyol. This may be attributed to greater thermal stability of ester linkages than ether linkages. It is also found from Table 4 that char residues of ester polyurethane and its composites were higher than that of ether-based polyurethane and its composites. Again, the values of T_2 for control materials were the same as for the clay-tethered composites, indicating that thermal stability does not depend on tethering effect as long as the clay particles are dispersed well.

3.6. Dynamic mechanical thermal analysis (DMTA)

Table 5 lists the values of dynamic storage modulus and soft segment T_g from the peaks of tan δ vs. temperature curves. An increase in soft segment T_g due to clay particles is observed only in the case of polyesterpolyol, where clay particles were in exfoliated state (Fig. 3(b)). In addition, approximately 36% increase in storage modulus over pristine TPU is seen for 5 wt% clay content. Recall, however, that T_g calculated from DSC data in Table 4 did not show dependence on clay content.

Table 6
Tensile properties

Material		Modulus (MPa)	Maximum stress (MPa)	Strain at break (%)
With polyether polyol	PU	0.22±0.005	0.81±0.028	900
	1 wt%	0.26±0.008	0.92±0.025	950
	3 wt%	0.49±0.041	1.14±0.073	1300
	5 wt%	0.62±0.052	1.31±0.033	1600
	Control	0.58±0.044	0.72±0.027	700
With polyester polyol	PU	0.79±0.021	2.38±0.077	1500
	1 wt%	1.17±0.079	3.18±0.134	2000
	3 wt%	1.60±0.147	4.32±0.158	2500
	5 wt%	2.09±0.151	5.39±0.497	3000
	Control	1.95±0.065	2.06±0.045	1200

3.7. Tensile properties

The values of tensile modulus, strength, and elongation at break of TPU and its nanocomposites are presented in Table 6. As a general trend, the values of tensile modulus increased with clay content. The values of tensile strength and elongation at break also increased with clay content. However, the control materials showed improvement only in tensile modulus. This, however, is not surprising, since the clay particles remained as micrometer size tactoids as seen in Fig. 3(c) and (d) and did not interact much with the polymer chains. Better dispersion and almost complete exfoliation of clay particles seen in Fig. 3(b) for composite of polyesterpolyol with 5 wt% clay yielded much better improvement in tensile properties than its polyetherpolyol counterpart—modulus, stress, and strain at break increased over TPU by 78, 125, and 100% respectively for polyesterpolyol compared to 64, 60, and 77% respectively for polyetherpolyol.

3.8. Tear strength

The values of tear stress, strain, modulus, and energy for break for TPU and its nanocomposites are presented in Table 7. As with tensile properties, polyesterpolyol nanocomposites also showed better tear strengths—the tear strength increased by 130% compared to 118% for ether-based nanocomposites with 5 wt% clay. The control materials, with no clay–polymer tethering, showed tear properties similar to TPU.

3.9. Abrasion resistance

Table 8 compares the loss of materials in abrasion tests. As a general trend, the loss of materials decreased with clay content and better performance was again observed in the case of polyesterpolyol based composites. The presence of 5 wt% clay led to a reduction in volume loss by 40% in polyetherpolyol composite and by 60% in polyesterpolyol composite. The abrasion resistance of control materials was slightly better than that of TPU.

4. Conclusions

The study, using higher molecular weight polyester and polyetherpolyol, endorsed the observations of an earlier study [23,24] that nanocomposites of TPUs with layered silicate clays are possible if clay–polymer tethering is allowed and if the shear stress during clay polymer mixing is high. In this study, nanocomposite was produced only in the case of polyesterpolyol due to much higher viscosity during clay–polymer mixing, although the extent of clay–polymer tethering was the same for both polyether- and polyesterpolyol. The study also showed that hydrogen bonding has no effect on mechanical properties and that clay particles

Table 7
Tear properties

Material		Modulus (MPa) ± standard deviation	Stress at break (MPa) ± standard deviation	Strain at break (%) ± standard deviation	Energy for break (J) ± standard deviation
With polyether polyol	PU	0.37 ± 0.003	0.53 ± 0.048	498 ± 10	0.27 ± 0.03
	1 wt%	0.60 ± 0.008	0.63 ± 0.036	502 ± 17	0.35 ± 0.03
	3 wt%	0.77 ± 0.062	0.96 ± 0.073	628 ± 10	0.78 ± 0.04
	5 wt%	1.27 ± 0.037	1.16 ± 0.036	827 ± 25	1.49 ± 0.11
	Control	0.79 ± 0.021	0.54 ± 0.018	387 ± 10	0.24 ± 0.01
With polyester polyol	PU	0.89 ± 0.021	1.18 ± 0.077	605 ± 10	0.76 ± 0.3
	1 wt%	1.57 ± 0.119	1.58 ± 0.028	750 ± 50	1.1 ± 0.21
	3 wt%	1.79 ± 0.369	2.04 ± 0.095	1517 ± 30	3.7 ± 0.09
	5 wt%	2.79 ± 0.105	2.76 ± 0.191	1780 ± 50	4.1 ± 0.06
	Control	2.00 ± 0.314	1.03 ± 0.092	521 ± 40	0.64 ± 0.11

Table 8
Abrasion test results

Material		Volume loss (cm^3/g)
With polyether polyol	PU	0.173
	1 wt%	0.167
	3 wt%	0.116
	5 wt%	0.098
	Control	0.148
With polyester polyol	PU	0.132
	1 wt%	0.118
	3 wt%	0.087
	5 wt%	0.054
	Control	0.105

showed no influence on hard segment hydrogen bonding. The presence of clay particles caused strong improvement in stability against thermal degradation, although clay–polymer tethering showed almost no effect. Clay tethering and resultant clay particles exfoliation, however, caused strong improvement in mechanical properties.

Acknowledgements

Partial financial support was obtained from National Science Foundation in the form of CAREER Award (DMI-0134106) to SCJ.

References

[1] Wang Z, Pinnavaia TJ. Chem Mater 1998;10:3769.
[2] Zilg C, Thomann R, Muelhaupt R, Finter J. Adv Mater 1999;11:49.
[3] Petrovic ZS, Javni I, Waddon A, Banhegyi G. J Appl Polym Sci 2000; 76:133.
[4] Chen TK, Tien YI, Wei KH. Polymer 2000;41:1345.
[5] Xu R, Manias E, Snyder AJ, Runt J. Macromolecules 2001;34:337.
[6] Ma J, Zhang S, Qi Z. J Appl Polym Sci 2001;82:1444.
[7] Tien YI, Wei KH. Macromolecules 2001;34:9045.
[8] Tien YI, Wei KH. Polymer 2001;42:3213.
[9] Hu Y, Song L, Xu J, Yang L, Chen Z, Fan W. Colloid Polym Sci 2001; 279:819.
[10] Yao KJ, Song M, Hourston DJ, Luo DZ. Polymer 2002;43:1017.
[11] Tien YI, Wei KH. J Appl Polym Sci 2002;86:1741.
[12] Chang JH, An YU. J Polym Sci, Part B: Polym Phys 2002;40:670.
[13] Tortora M, Gorrasi G, Vittoria V, Galli G, Ritrovati S, Chiellini E. Polymer 2002;43:6147.
[14] Zhang X, Xu R, Wu Z, Zhou C. Polym Int 2003;52:790.
[15] Song M, Hourston DJ, Yao KJ, Tay JKH, Ansarifar MA. J Appl Polym Sci 2003;90:3239.
[16] Mishra JK, Kim I, Ha CS. Macromol Rapid Commun 2003;24:671.
[17] Chen X, Wu L, Zhou S, You B. Polym Int 2003;790.
[18] Rhoney I, Brown S, Hudson NE, Pethrik RA. J Appl Polym Sci 2003; 91:1335.
[19] Osman MA, Mittal V, Morbidelli M, Suter UW. Macromolecules 2003;36:9851.
[20] Kojima Y, Usuki A, Kawasumi M, Okada A, Fukushima Y, Kurauchi T, et al. J Mater Res 1993;8:1185.
[21] Fukushima Y, Okada A, Kawasumi M, Kurauchi T, Kamigaito O. Clay Miner 1998;23:27.
[22] Cao X, Lee LJ. SPE ANTEC Proc 2004;1896.
[23] Pattanayak A, Jana SC. Polymer 2005;46:3275.
[24] Pattanayak A, Jana SC. Polymer 2005;46:3394.
[25] Pattanayak A, Jana SC. Polym Eng Sci, accepted for publication.
[26] Sung CSP, Schneider NS. Macromolecules 1975;8:68.
[27] Mille JA, Lin SB, Hwang KS, Wu KS, Gibson PE, Cooper SL. Macromolecules 1985;18:32.
[28] Koberstein JT, Russel TP. Macromolecules 1986;19:714.
[29] Lee HS, Wang YK, Hsu SL. Macromolecules 1987;20:2089.
[30] Lee HS, Wang YK, Macknight WJ, Hsu SL. Macromolecules 1988; 21:270.
[31] Coleman MM, Lee KH, Skrovanek DJ, Hu J, Painter PC. Macromolecules 1986;19:2149.
[32] Srichatrapimuk VW, Cooper SL. J Macromol Sci, Phys 1978;B15: 267.
[33] Senich GA, Macknight WJ. Macromolecules 1980;13:106.
[34] Velankar S, Cooper SL. Macromolecules 1998;31:9181.
[35] Yoon PJ, Han CD. Macromolecules 2000;33:2171.
[36] Ryan AJ, Macosko CW, Bras W. Macromolecules 1992;25:6277.
[37] Coleman MM, Lee KH, Skrovanek DJ, Painter PC. Macromolecules 1986;19:2149.
[38] Wang TL, Hsieh TH. Polym Degrad Stab 1997;55:95.
[39] http://www.nanoclay.com/data/30B.htm.